Catena 249 (2025) 108605

Contents lists available at ScienceDirect

Catena

journal homepage: www.elsevier.com/locate/catena

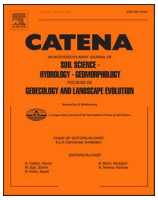

Understanding the geochemical composition of alluvial sediments in a complex environmental system – A case study of the Mura/Mur river

Čeplak Barbara [a], Moser Ulrike [b], Irrgeher Johanna [b], Šala Martin [c], Kralj Polona [a], Žibret Gorazd [a,*]

[a] Geological Survey of Slovenia, Dimičeva ulica 14, 1000 Ljubljana, Slovenia
[b] Montanuniversität Leoben, Chair of General and Analytical Chemistry, Franz–Josef–Strasse 18, 8700 Leoben, Austria
[c] National Institute of Chemistry, Hajdrihova ulica 19, 1000 Ljubljana, Slovenia

ARTICLE INFO

Keywords:
Factor analysis
River sediments
CIA
PIA
ICV
Geochemistry
Particle characterization

ABSTRACT

The study provides a comprehensive investigation of the geochemical properties of stream and alluvial sediments in an area characterised by a complex natural (geochemical) and anthropogenic environment of the transboundary Mura River (Austria, Slovenia, EU). A total of 65 sediment samples from active river channel and tributaries, and 59 samples from 6 floodplain sediment profiles were collected and analysed. ICP–MS analysis was used to determine the levels of 59 elements in two fractions (<0.063 and 0.063–0.125 mm). Natural (geological) and anthropogenic factors influencing the elemental composition were determined. The sediments showed a low degree of weathering in the upper part of the river and a moderate degree in the middle and lower parts. They are enriched with As, Co, Cr, Cu, Mo, Ni, and Sb compared to the median values for the European stream and floodplain sediments. This can be a consequence of the presence of natural ore mineralisation in Upper Styria along with related lithological features. Factor analysis revealed four natural geochemical associations (K–Ba–Rb–Ga–Li–Tl–Cs–Be–Al–Cu–V; Th–YREE–U; Zr–Hf–Nb; Na–Sr), one anthropogenic association (Cd–In–Zn–Pb) and two combined (geogenic and anthropogenic) associations (Ni–Cr–Mg–Co–V and Fe–Sc–Ti–Nb). Particle analysis by SEM/EDS was used to identify characteristic carriers of specific elements and potentially to determine their sources.

1. Introduction

Rivers have always played a pivotal role in the development of cities and civilizations throughout human history. They provide water and serve as a means of transportation, while alluvial areas have been used for agriculture and animal domestication. The long–term use of river water and floodplains, from the beginning of human civilization to the present, along with natural changes, is reflected in the geochemical composition of river basins worldwide (Hoffmann et al., 2010). Rapid industrialization, extensive agriculture, traffic, mineral extraction, and infrastructure development have increased the levels of potentially toxic elements (PTEs) in alluvial sediments. In recent years several studies have addressed the PTE levels in various media, including soils (Pučko et al., 2024), plants (Barandovski et al., 2020), urban sediments (Gaberšek and Gosar, 2021; Teran et al., 2020) water (Lychagin et al., 2015; Rieuwerts et al., 2014), river sediments (Kos et al., 2022; Reese et al., 2019; Žibret and Čeplak, 2021) and other environments.

Alluvial sediments act as a sink for pollutants, while floodplain sediments represent an archive of their historical composition (Žibret and Gosar, 2017). Erosion and transportation of materials within river channels is one of the most important natural transport pathways (Meybeck, 1976). Depending on the particle size, rivers can transport and sort pollutants over various distances, even up to 500 km from their source (Foucher et al., 2009). Under favorable conditions in terms of redox potential, pH, dissolved oxygen, and temperature, trace elements can be released into the water, posing a potential risk to aquatic ecosystems, groundwater, and inhabitants through the food chain (Cheng et al., 2013). For this reason, understanding the background levels of elements in a given area is crucial, as it enables the distinction between natural and anthropogenic anomalies. It also provides insight into the source material, chemical and physical conditions in an area, the geo–tectonic environment, climate changes (Verma et al., 2022), and serves as an indicator of possible anthropogenic activities over time (Briffa et al., 2020).

* Corresponding author.
E-mail address: gorazd.zibret@geo-zs.si (Ž. Gorazd).

https://doi.org/10.1016/j.catena.2024.108605
Received 5 August 2024; Received in revised form 22 November 2024; Accepted 24 November 2024
Available online 5 December 2024

The geochemical composition of sediments is influenced by various factors, such as the type of source material (bedrock), topography, climatic conditions, degree of weathering, and transport mechanisms (Gosar and Žibret, 2011; Reczyński et al., 2020). This makes rivers a complex system that interacts with a range of natural elements and, in recent geological history, anthropogenic factors. The latter is also the case for the Mura River, which exhibits significant differences in morphology, population density, land use, and lithology throughout its course. Sediments from the catchment area have been influenced by past and present mining and smelting activities (Schimak et al., 2005), industry, agricultural activities, and urbanization. There are more than 30 run–of–river hydropower plants on the Austrian side, and the river banks have undergone extensive construction throughout history, resulting in a lowered riverbed and groundwater levels (Globevnik and Mikoš, 2009). Considering all of these features, the Mura River serves as a good example of a highly complex fluvial environment.

The study's objectives are to determine the geochemical associations of elements in such a complex environment, to possibly distinguish between natural (background values) and anthropogenic associations, and eventually identify their sources. This information is an important basis for sustainable management of transboundary rivers, land use planning on alluvial plains and the protection of groundwater. It can also provide valuable baseline data in the event of potential future environmental accidents or emissions. The methodology used in this case study can be applied to other similar environments worldwide. Additionally the collected data can be used for the future development of global and regional background values for alluvial materials, and can serve as a basis for comparison with other complex river systems around the globe.

2. Materials and methods

2.1. Geographical and geological setting

The Mura is a Central European river that is part of the Black Sea watershed. Its source lies at the altitude of 1898 m in the Hohe Tauern in Austria. The river is known by two names, the Slovenian "Mura" and the Austrian "Mur". In this study, the Slovenian "Mura" will be used throughout the text.

In the upper parts, the Mura River meanders and flows continuously, making it a perennial waterway. Initially, it flows towards the west and

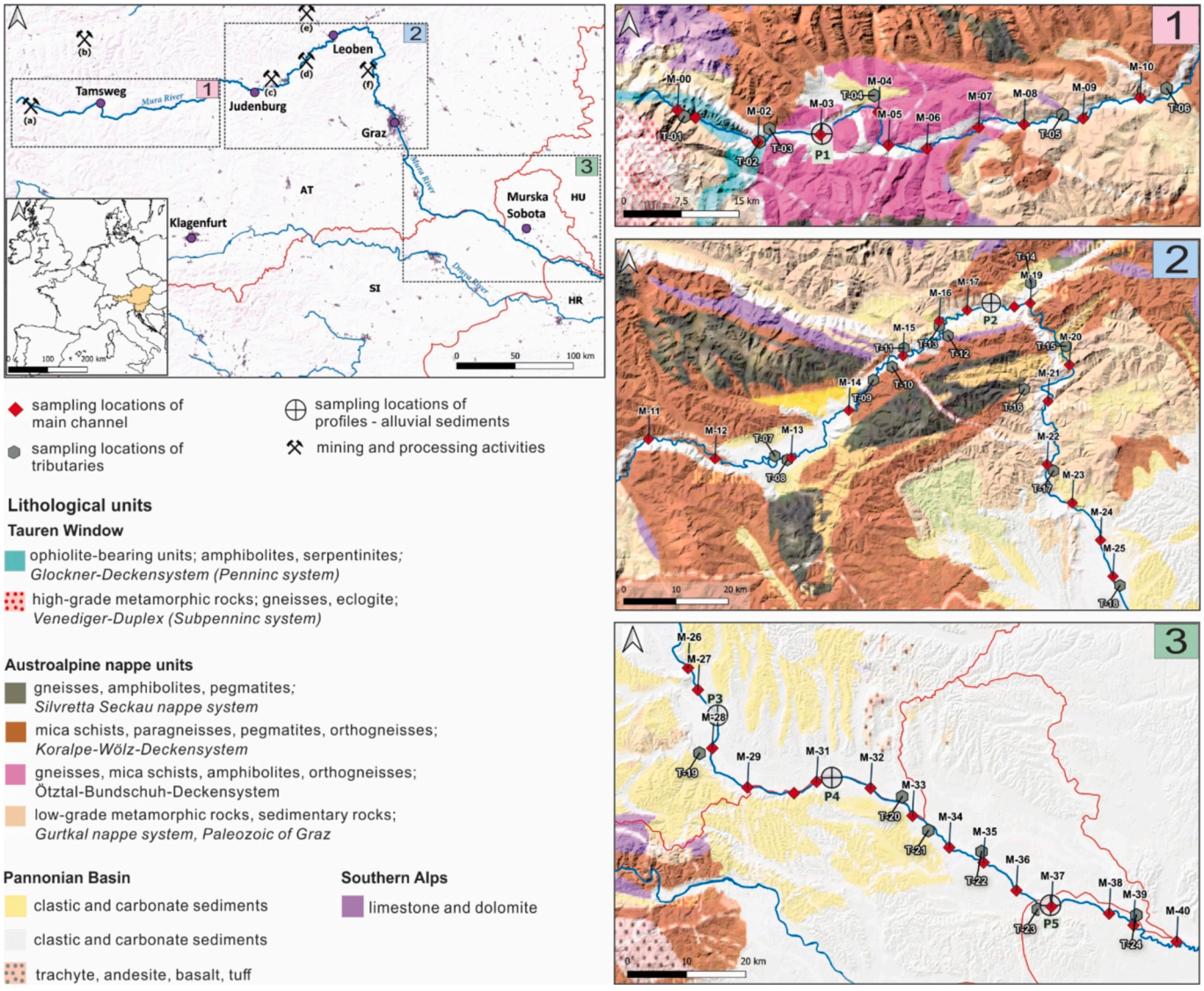

Fig. 1. Simplified geological map of the investigated area with sampling locations and major mining activities: 1. Zone 1 – high–grade metamorphic rocks; 2. Zone 2 – lower grade metamorphic rocks; 3. Zone 3 – Neogene sediments of the Pannonian Basin and outcroppings of Pliocene alkali basaltic volcanic rocks (Source: OneGeology GISEurope Bedrock and Structural geology, SRTM 90 m DEM); major mining locations: (a) As–Au–Ag mine Rotgulden, (b) Ag–Ni mine Obertal, (c) Cu–Au mine Flatschach, (d) Kraubath area, (e) Fe mine Erzberg and (f) Pb–Zn mine Arzwaldgraben.

northwest and follows the Mur–Mürz fault line which is one of the dominant tectonic structures of the Alps. At the Bruck an der Mur, the river turns sharply south towards the city of Graz. In this section the river flow is antecedent, and the meanders are not well expressed. At the town of Graz, it reaches the Pannonian Basin and starts flowing towards SE, with well–developed meanders, riverbanks, dead channels, oxbow lakes, etc. At the altitude of 130 m the river effluents with the Drava River. Its average gradient is 3.81 m/km, and the mean discharge at the water monitoring station at Gornja Radgona in 2021 was 114 m^3/s (Strojan, 2022).

From the geological perspective, the study area can be divided into three distinct zones: Zone 1, Zone 2, and Zone 3 (Fig. 1). Zone 1 represents the uppermost part of the Mura catchment and is composed of high–grade metamorphic rocks of the Tauren window (schists, gneiss, eclogite etc.; Schmid et al., 2013). The middle part (Zone 2) is geologically the most heterogeneous and consists of the Austroalpine nappe system which is subdivided into several nappe subsystems i.e., Silvretta–Seckau, Koralpe–Wölz, Ötztal–Bundschuh, and Drauzug–Gurktal. They consist of various metamorphic rocks of the Paleozoic, sedimentary and volcanic rocks of the Permian and Mesozoic, with igneous intrusions (granites) of the Tertiary (Gasser et al., 2009). The lowest part (Zone 3) belongs to the Pannonian Basin, which is mostly filled with clastic rocks and sediments ranging in age from the Neogene to the Quaternary, together with outcrops of the Pliocene alkali–basaltic volcanic rocks (Kralj, 2011).

2.2. Sampling and sample preparation

The term “stream sediments” is used for fine–grained sediments that were deposited within the active river channel during the last high–water event, while the term “alluvial sediments” is used for fine–grained sediments which were deposited outside the active river channel on the floodplains. Samples of stream and alluvial sediments were collected between August 2022and November 2023. In total 41 samples of stream sediments from the main river channel (labelled: M−00 (uppermost sample) to M−40 (lowermost sample)), 24 stream sediments from larger tributaries (labelled: T–01 to T–24) and 62 samples of alluvial sediments (labelled as A) from six profiles (P1, P2–FP, P2–T1, P3, P4, P5) were collected. Detailed information about sampling points is presented in the supplementary material, Table S1. Stream sediment samples were collected with a plastic spatula and plastic bag, secured with rubber bands as a composite sample from at least 5 different microlocations in the radius of 100 m inside the inner convex river band. The spatula was cleaned between samples to prevent cross–contamination. The distance between sampling points was between 7 to 13 km. Stream sediments from tributaries were collected using the same method as those from the main river channel. The samples were taken near the confluence with the Mura River, but ensuring they were far enough away to avoid being influenced by the main river.

Alluvial sediment profiles were collected on active floodplains in the vicinity of the main river channel. Only one profile, P2–T1, was sampled on the 1st river terrace. Initially, a hole with dimensions of 30 x 30 x 20 cm was excavated with a shovel and a vertical hole with a diameter of approximately 5 cm was drilled with a hand auger. Samples were taken every 20 cm until the gravel layer was reached. The depth of profiles varied between 50 and 240 cm. Samples from the first 20 cm (i.e., 0–5 cm, 5–10 cm, 10–20 cm) were collected separately with a plastic spatula. Approximately 0.5 kg of each sample was collected from each spot and stored in pre–labelled bags. All samples were air–dried in an oven at 303 K until a constant weight was obtained. Plant remains, rocks, and other debris were removed, while potential aggregates were gently crushed in ceramic mortar. Sediment samples were sieved using 0.125 and 0.063 mm meshes to obtain pulps for the determination of elements.

2.3. Analytical methods

The determination of 59 elements in two fractions (<0.063 mm and 0.063–0.125 mm) was conducted in the external commercial laboratories of Bureau Veritas Mineral Commodities Laboratories, Vancouver, Canada, according to the international standards ISO 9001:2008 using inductively coupled plasma mass spectrometry (ICP–MS) after near total digestion method (analytical package MA250). 0.25 g of the material was heated in HNO_3, $HClO_4$ and HF to fuming and then dried, and the residue was then dissolved in HCl.

The precision and accuracy of the elemental analysis were controlled by 32 duplicates and 46 measurements of 8 different reference materials (SdAR–L2–RM, SdAR–H1–RM, SdAR–M2, OU–6, OREAS45F, OREAS45H, OREAS501D and OREAS25A–4A). Measurements below the detection limit were estimated with 50 % of the corresponding lower detection limit. Elements (i.e. Re and S), where corresponding elemental levels were below the detection limit in more than 30 % of the samples, were excluded from further analysis.

Four selected samples of stream sediments were selected to determine mineral composition (M−03, M−15, M−24, and M−39). PANalytical Empyrean X–ray diffractometer equipped with CuKα radiation with $\lambda = 1.54$ Å was used. Samples were scanned at 40 mA and a voltage of 45 kV over the 2θ range from 4° to 70°, with a step size of 0.013° 2θ and a scan step time of 69 s. PANalytical X'Pert High Score Plus diffraction software (v.4.1.0.19887) was used to determine phase composition using the ICSD FIZ Karlsruhe2014–1 database.

To further support conclusions based on elemental and mineralogical analysis, selected samples were inspected with Scanning electron microscopy with Energy Dispersive Spectroscopy (SEM/EDS) using a JEOL JSM 6490LV SEM coupled with an Oxford INCA PentalFETx3 Si(Li) detector and INCA Energy 350 processing software at 20 keV accelerating voltage and 10 mm working distance. Individual particles, which are the main carriers of specific elements, were analysed for their size, composition, and shape.

2.4. Calculation of enrichment factors and indices

The enrichment ratios (ER_{EU}) were calculated by using the corresponding European median values for sediments; i.e. stream and floodplain sediments (Salminen et al., 2005) for fraction < 0.063 mm. As a rule, the elemental levels are compared with a reference element that has low mobility and is characteristic of natural sources. The most suitable reference elements include Al, Fe, Mn, Rb, and Ti (Žibret and Rokavec, 2010). Al was used as a normalizing element as the most suitable one for the study area, because it is the least likely that its levels in sediments are influenced by anthropogenic activities. The ER_{EU} calculations were performed according to the following equation: $ER_{EU} = [(C_{x(measured)})/(C_{ref/(measured)})] / [C_{x(backg.)} / C_{ref(back)}]$.

Where $C_{x\ (measured)}$ means the levels of a selected chemical element measured on a selected sampling location, $C_{ref\ (measured)}$ means the level of reference element (i.e. Al) measured on a specific sampling location, $C_{x\ (backg.)}$ represents the background level of one chemical elements, $C_{ref\ (backg.)}$ represents the background level of a reference chemical element. EF_{EU} values below 2 represent no enrichment (Sutherland, 2000).

The enrichment of elements in smaller fraction (ER_{fr}) was calculated by comparing median values in coarser fraction ($Md_{0.125–0.063}$) with smaller one ($Md_{<0.063}$) according to the equation: $ER_{fr} = Md_{0.125–0.063} / Md_{<0.063}$.

The degree of chemical weathering was evaluated according to the Chemical Index of Alteration (CIA) (Nesbitt and Young, 1989), where $CIA = (Al_2O_3 / (Al_2O_3 + CaO^* + Na_2O + K_2O)$ x 100. CaO* is the amount of CaO incorporated in the silicate fraction of parent rocks calculated as $CaO^* = CaO - 10/3 * P_2O_5$. If the calculated CaO* was less than the amount of Na_2O, the CaO* values were applied. In case the calculated CaO* exceeds Na_2O, the amount of Na_2O was used (McLennan, 1993). The CIA values in a range between 45 and 55 indicate no chemical

weathering, values between 60 and 80 indicate moderate chemical weathering, and values above 80 imply intensive chemical weathering.

Weathering intensity was calculated using the Plagioclase Index of Alteration (PIA; Fedo et al., 1995) in accordance with the following equation: PIA = 100 x [($Al_2O_3 - K_2O$) / ($Al_2O_3 + CaO^* + Na_2O + K_2O$)]. Unweathered plagioclase feldspar has a PIA value of 50, while aluminous clay minerals reach the highest PIA value of 100.

The Index of Compositional Variability (ICV) serves as an indicator of weathering resistance (Cox et al., 1995). The following formula was used to calculate ICV: (Fe2O3 + Na_2O + K_2O + CaO^* + MgO + TiO_2) / Al_2O_3. High ICV values of sediments (> 0.84) reflect sediment immaturity, whereas low ICV values indicate highly weathered sources (Cox et al., 1995; Hossain et al., 2018).

2.5. Statistical methods

Geochemical associations of elements were determined according to the factor analysis (FA), by using Statistica 13 software (TIBCO Software Inc., 2020). The application of FA has been shown to be a useful method for determining the connection between major and trace elements in several studies (Mil-Homens et al., 2013; Popov et al., 2014). 254 analyses of elemental levels in stream sediments of the main river channel, tributaries, and alluvial profiles in two fractions were considered. Seven factors were extracted. Elements that tended not to be loaded in any of the seven factors were excluded from the factor analysis (Ag, As, Bi, Ca, Mg, Mn, Mo, P, Sb, Se, Ta, Te, and W). 30 elements or groups of elements were retained: Al, Ba, Be, Cd, Co, Cr, Cs, Cu, Fe, Ga, Hf, In, K, Li, Na, Nb, Ni, Pb, Rb, Sc, Sr, Th, Ti, Tl, U, V, YREE, Zn and Zr. YREE means the sum of all rare earth elements and yttrium. Factor analysis was performed on logarithmically transformed data.

3. Results

3.1. Distribution of chemical elements in stream sediments

Fig. 2 and Table S2 from supplementary material show the descriptive nonparametric statistics, the results of the analytical quality control and enrichment ratios ER_{EU} and ER_{fr} of 57 chemical elements. The quality of elemental analyses was found satisfactory for the majority of elements, except for Mo, Se, Te, and W where average deviations of replicates (ARPD) exceed 15 %.

The values of the ER_{EU} parameter show that elements in stream and alluvial sediment of the Mura River are generally comparable to the corresponding median values of sediments in Europe (EU_{med}), with the exception of As, Co, Cr, Mo, Ni, and Sb in stream sediments and As, Co, Cu, and Ni in alluvial sediments (Table S2 from supplementary material), in which the ER_{EU} are more than 3. ER_{fr} values indicate that elemental enrichments are greater in finer fractions compared to coarser

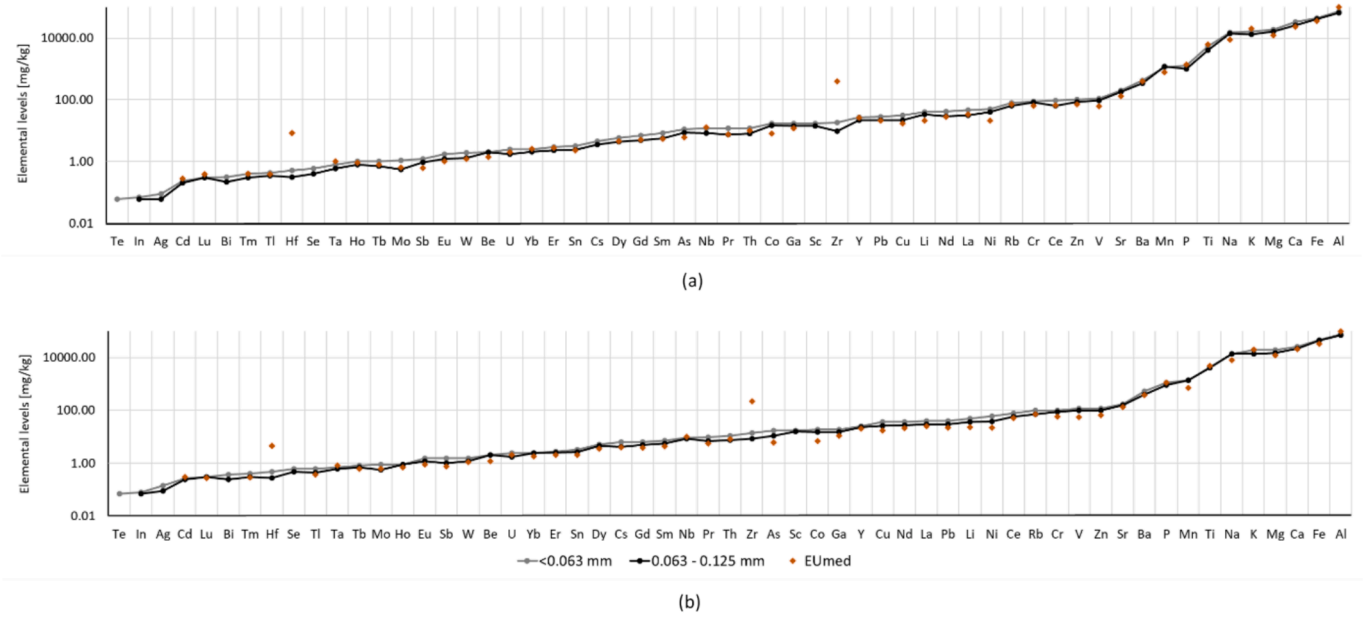

Fig. 2. Median values of chemical elements in (a) stream and (b) alluvial sediments in comparison with corresponding EU median values in the <0.063 and 0.063–0.125 mm fractions.

Table 1
Mineralogical composition of selected samples as determined by Rietveld refinement (wt. %) and goodness of fit parameter from global variables list in X'Pert High Score Plus program.

mineral	Formula	M−03	M−15	M−24	M−39
quartz	SiO_2	32.4	38.0	26.2	39.3
muscovite / illite	$(KF)_2(Al_2O_3)_3(SiO_2)_6(H_2O)$ / $(K,H_3O)(Al,Mg,Fe)_2(Si,Al)_4O_{10}[(OH)_2,(H_2O)$	11.2	12.4	8.7	22.8
albite	$NaAlSi_3O_8$	15.1	25.5	18.4	19.1
dolomite	$CaMg(CO_3)_2$	24.3	5.3	20.1	9.2
chlorite group of minerals	$(Mg, Fe, Li)_6AlSi_3O_{10}(OH)_8$	10.0	1.3	9.2	6.6
hornblende	$(Ca,Na)_2(Mg,Fe,Al)_5(Al,Si)_8O_{22}(OH,F)_2$	2.3	10.6	3.6	3.0
K–feldspar	e.g. orthoclase [$KAlSi_3O_8$]			7.4	
calcite	$CaCO_3$	4.7		6.4	
garnet group of minerals	e.g. almandine [$Fe_3Al_2Si_3O_{12}$]		6.8		
sum	/	**100**	**100**	**100**	**100**
goodness of fit		**5.5**	**4.0**	**10.9**	**5.4**

ones, except for Mn in stream and Na in alluvial sediments.

Table 1 presents the mineralogical composition of selected stream sediment samples (M−03, M−15, M−24, and M−39) determined by Rietveld refinement. The main mineral phases of all samples are quartz, Na–plagioclase, muscovite/illite, dolomite, chlorite, and hornblende, while phases such as K–feldspar, calcite and minerals of the garnet group are contained only in a few samples.

Various geochemical indices were used to assess the weathering intensity of the Mura sediments (Fig. 3a, Table S3 from supplementary material). The CIA values are relatively low and range between 53 and 71 (average 62), indicating moderate chemical weathering. The lowest CIA values were measured in Zone 1, while the highest were measured in the Ščavnica tributary (T–23) in the lower part of the river. The major oxide composition of the main river channel samples presented in the ternary diagram (e.g. Fig. 3a) Al_2O_3 – (CaO* + Na_2O) – K_2O (A–CN–K) reveals that the corresponding data points are distributed in a small area with a slight trend towards the muscovite/illite component for the Zone 3. In contrast, the corresponding data points for the alluvial and tributary stream sediments are more widely dispersed and show a stronger tendency towards the muscovite/illite component than stream sediments of the main channel. The PIA values, which range from 54 to 82 with an average value of 68, are generally consistent for the main channel stream sediments. In contrast, the alluvial and tributary stream sediments exhibit a wider range of values. The values of the CIA/PIA diagram (Fig. 3b) show an intermediate weathering of plagioclase especially in zones 2 and 3. The ICV values range between 1.2 and 3.3, with an average value of 1.6 indicating low weathering of the parent material in the source region. The comparison of CIA and ICV (Fig. 3c) suggests that the sediments of the Mura River are immature in their composition. The exact contents of the most important oxides are listed in Table S3.

Table 2 presents the factor loadings for each of the seven extracted factors. Varimax raw factorial axes rotation was used. Factor analysis explains a total of 90 % of all variances for the elements mentioned above. Fig. 4 shows factor score distribution for stream sediments of the Mura River for both fractions together with a polynomial trendline. Factor score values are generally higher in smaller fractions.

Factor 1 (F1), which is the strongest factor, explains 30 % of the total variance. The following elements are loaded in F1: K, Ba, Rb, Ga, Li, Tl, Cs, Be, Al, Cu, and V. Although F1 score values vary significantly throughout the river course, they are generally the highest in the uppermost part of the river. Factor 2 (F2) explains 13 % of the total variance and is associated with Ni, Cr, Mg, Co, and V. The highest F2 scores, especially in smaller fractions, were detected in tributary Chromwerkgrabenbach (T–09), which flows into the Mura River in the area of Zone 2, 175 km downstream from its source. High values were also detected in sediments of tributaries Rantenbach (T–05), Lobmingbach (T–10) and Raababach (T–18). Factor 3 (F3) is loaded with Fe, Sc, Ti, and Nb and represents 11 % of the total variance. The highest F3 scores were detected in coarser fractions in sediments of Zederhausbach (T–03), Taurach (T–04), and Gamsgraben (T–16) tributaries, as well as in the area of Sankt Michael in der Obersteirmark (M−15) and Niklasdorf (M−17). A significantly high F3 value was also detected in Zone 3 in the sediments of the Ščavnica (T–23) tributary. Th, YREE, and U are loaded

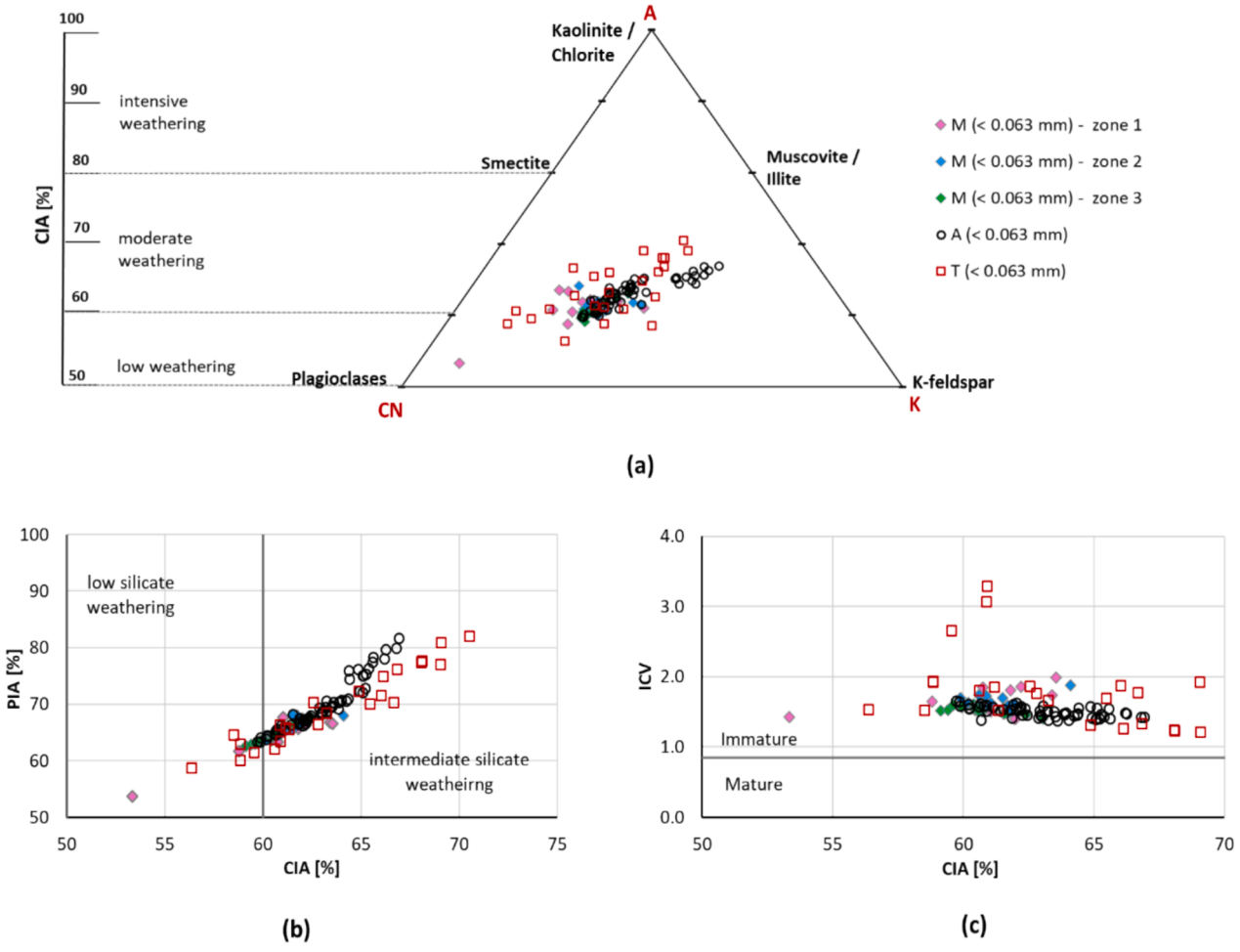

Fig. 3. a) CIA (Chemical Index of Alteration) values and A–CN–K ternary diagrams of the stream (M – Mura River, T – tributary) and alluvial (A) sediments. Symbols on the edges of triangle: A = Al_2O_3, CN = CaO* + Na_2O, K = K_2O; b) CIA vs. PIA (Plagioclase Index of Alteration); c) CIA vs. ICV (Index of Compositional Variability).

Table 2
Factor loadings (values below 0.5 are not shown).

	F1	F2	F3	F4	F5	F6	F7	VAR
K	0.94							97
Ba	0.92							94
Rb	0.91							93
Ga	0.90							95
Li	0.89							90
Tl	0.89							96
Cs	0.89							95
Be	0.85							76
Al	0.79							95
Cu	0.67							86
V	0.57	0.50						87
Ni		0.90						93
Cr		0.89						87
Mg		0.85						78
Co		0.81						96
Fe			0.92					95
Sc			0.77					95
Ti			0.70					91
Th				0.93				94
YREE				0.87				95
U				0.83				82
Zr					0.93			97
Hf					0.91			92
Nb			0.55		0.61			90
Cd						0.89		90
In						0.77		72
Zn						0.72		89
Pb						0.71		76
Na							0.85	90
Sr							0.77	90
Expl.Var	8.9	3.8	3.2	3.2	2.9	2.8	2.2	
Prp.Totl	30	13	11	11	10	9	7	90

EL – element; F1–F7 – factors; VAR – explained variance. Expl.Var – strength of the factor represented by eigenvalue; Prp.Totl – explained total variance by individual factor in %.

in factor 4 (F4), which explains 11 % of the total variance. F4 scores are generally higher in Zone 1, especially in smaller fractions. Higher values of F4 score were also detected in sediments of the main channel in St. Michael in der Oberstermark (M−15) and tributaries Granitzenbach (T–08) and Liesing (T–11), all located in Zone 2. Another slight increase in F4 scores is observed in sediments of tributary Sulm (T–19) near the Austrian–Slovenian border. Factor 5 (Zr, Hf, Nb; F5) represents 10 % of the total variance. The F5 score values show an increasing trend along the Mura River with higher values predominantly observed in smaller fractions. Factor 6 (F6) explains 9 % of the total variance and is loaded with Cd, In, Zn and Pb. Generally, the highest values of F6 scores are characteristic of the historical mining and urbanized areas; Schellgaden (M−02), Leoben (M−16), and Graz (M−24) as well as in several tributaries such as Zederhausbach (T–03), Wölzer Bach (T–06), Rötschbach (T–17), and Ledava (T–24). The last factor, factor 7 (F7), is loaded with Na and Sr and explains 7 % of the total variance. The highest F7 scores were found in Zone 1. Significantly higher F7 score values were also found in a coarser fraction of the tributaries Wölzer Bach (T–06) and Drauchenbach (T–20).

Fig. 5 presents the distribution of factor scores in the alluvial sediment profiles for both fractions. Similar to stream sediments, the highest F1 scores are found in P1 from Zone 1. P1 also has the highest F2 values. Particularly high values of this factor in coarser fractions were found at a depth of 160 cm. The F3 scores are the highest in the small fraction on the terrace profile P2–T1, while for the coarser fraction, the highest factor scores were found at P5 at a depth of 140 cm. Significantly high F3 score values in the coarser fraction were also found in P3 at a depth of 50 cm. As with the stream sediments, the F3 scores are also higher in the coarse fraction of the alluvial sediments. The values of F4 scores are the highest in the coarser fraction in the lower part of profile P5 and in the stream sediments of the Sulm (T–19) tributary. Although the values of F4 in the coarser fraction are generally lowest at P1, a significantly high value was found in the sediments at a depth of 180 cm. A similar pattern can also be observed in the finer fraction, where the highest values for F4 were found in P2–FP. The values for F5 are the lowest in the P1 for both fractions, while in the other profiles, these values are generally similarl. This is consistent with the observations in the stream sediments where the lowest F5 scores were identified in Zone 1. High F6 score values were observed in the upper parts of profiles P3, P4, and P5 in both fractions. The F7 scores are the lowest at profile P1 and highest at profiles P2–FP and P2–T1. This tendency is particularly evident in the smaller fraction compared to the coarser fraction.

SEM/EDS was used to identify mineral grains that are characteristic carriers of elements grouped into individual factors. The focus was placed on elements with elemental levels high enough to allow the detection of individual element–bearing carriers under SEM. Potential corresponding mineral phases of individual grains from SEM images were assumed exclusively on the basis of the EDS spectra. For the actual determination of mineral phases, other mineral identification methods should be used (i.e. XRD or EBSD). The most representative element for F1 is K. Samples from the uppermost part of the river (M−00 to M−03) contain abundant mica grains (e.g. muscovite) which are carriers of K, as well as of Al and Li (Fig. 6a). In those samples, barite particles were also recognized as carriers of Ba, which is also loaded in F1. Barite grains are between 2 and 10 μm commonly of anhedral shape. Occasionally, particles with relatively sharp edges were also detected (Fig. 6b). SEM/EDS analysis was focused on Cr–Ni bearing particles because these two are the most representative elements for F2. Cr–Ni–bearing particles from the Mura tributary Chromwerkgrabenbach mostly occur as Cr–spinels, occasionally with traces of Ti, Mg, and Zn, while individual Ni–bearing particles were rarely identified. Grains of Cr–spinels are rounded to partly rounded (Fig. 6c), sporadically with cracked surfaces, however, grains with sharp edges were also detected. Their mean size ranges from 10 to 80 μm. Fe–oxyhydroxides with minor content of Ni occur as anhedral fragments with minute crystallites in size of 15 μm (Fig. 6d). Fe and Ti are characteristic elements for F3. Grains of Fe–oxyhydroxides and Ti–bearing minerals (e.g. ilmenite, titanite, rutile) are very common in all observed samples. Ilmenite and titanite grains are mostly subhedral in shape although euhedral grains can also occur. TiO_2 (probably rutile) mostly appears in an elongated shape with a relatively smooth surface, occasionally as an intrusion on ilmenite grains (Fig. 6e). One of the most commonly found minerals in observed samples with high F3 scores is pyrite (FeS_2), which usually occurs as euhedral cubic grains – framboidal pyrite in size up to 8 μm (Fig. 6f). High values of F3 could also be linked to the presence of Fe–rich garnets, which are abundant in sample M−15. These grains typically have sharp edges and are approximately 80 μm in size (Fig. 6g). Sediments of the Mura River also contain several REE–bearing minerals (F4), such as monazite and xenotime group minerals. These grains usually have anhedral shapes and are only few μm in size (Fig. 6h). However, in the case of monazite, subhedral grains up to 60 μm were also identified (Fig. 6i).

Zr is the most representative element for F5, and carriers of this element are usually zircon crystals. Euhedral prismatic (Fig. 6j) grains with a size from a few μm up to 20 μm predominate, while occasionally subhedral and rounded zircon particles are also present. Zn and Pb are the two most characteristic elements of F6. Carriers of these two elements are Fe–oxyhydroxides with traces of Mn, Zn, Cu, and Pb sulphides. Particles are either spherical or irregularly shaped. EDS spectres show that spheres mainly contain Fe and O with traces of Al and Si as well as various PTEs such as Zn, Cu, Cr, and Mn (Fig. 6k, 6l). Irregular Fe oxyhydroxides with minor amounts of Zn and Cu occasionally exhibit bubble–shaped perturbances (Fig. 6m). Pb–oxides and sulphides occur as small angular fragments, approximately 2 μm in size (Fig. 6n). Apatite is a common mineral found in observed samples and may also carry PTEs such as Cd, Pb, and Zn. Apatite grains usually appear as euhedral or

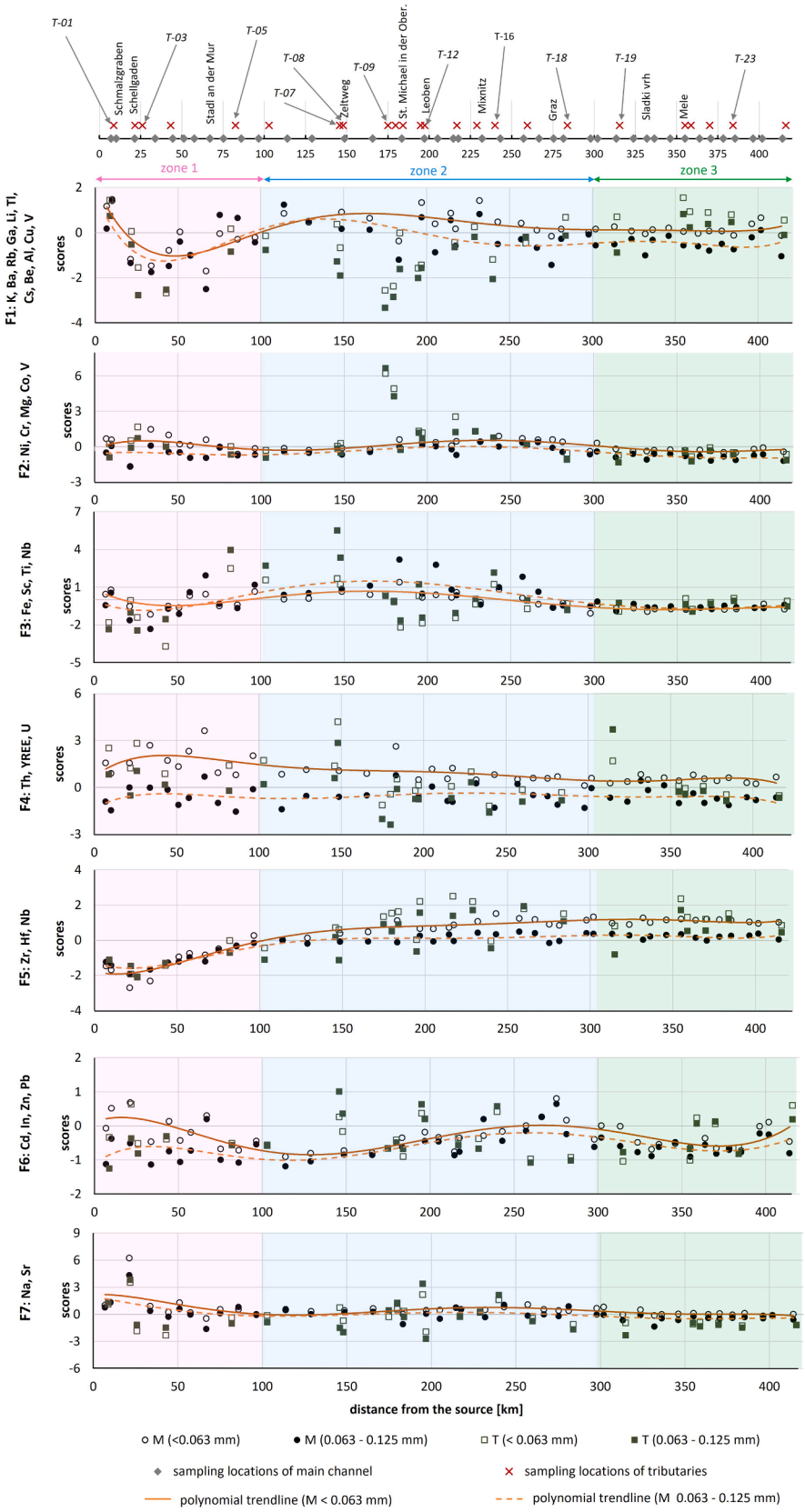

Fig. 4. Factors score values (F1–7) in stream sediments from the main channel (M) and tributaries (T) in both fractions.

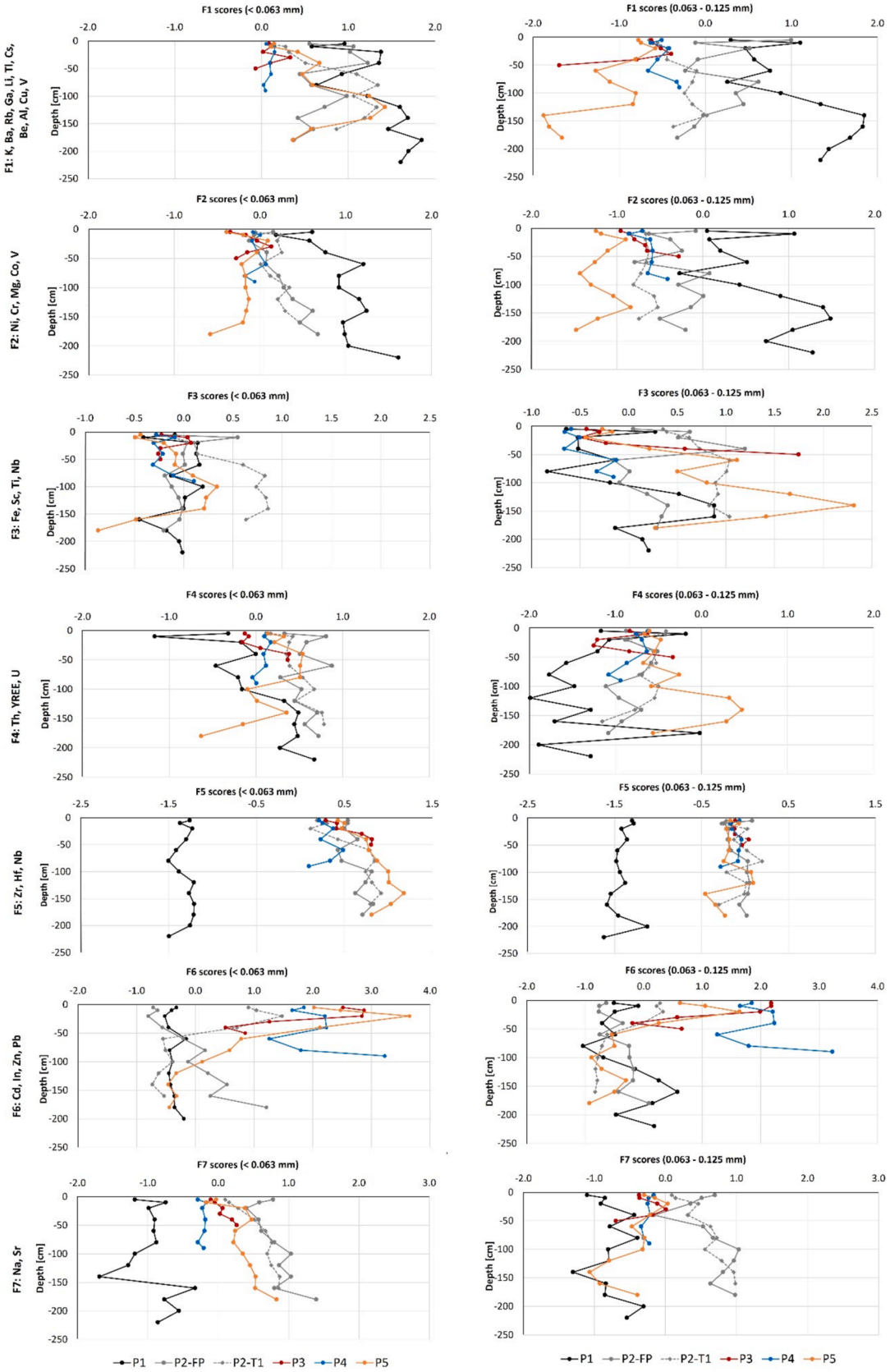

Fig. 5. Factors score values (F1–7) in profiles (P) through alluvial sediments for fractions <0.063 mm and 0.063–0.125 mm.

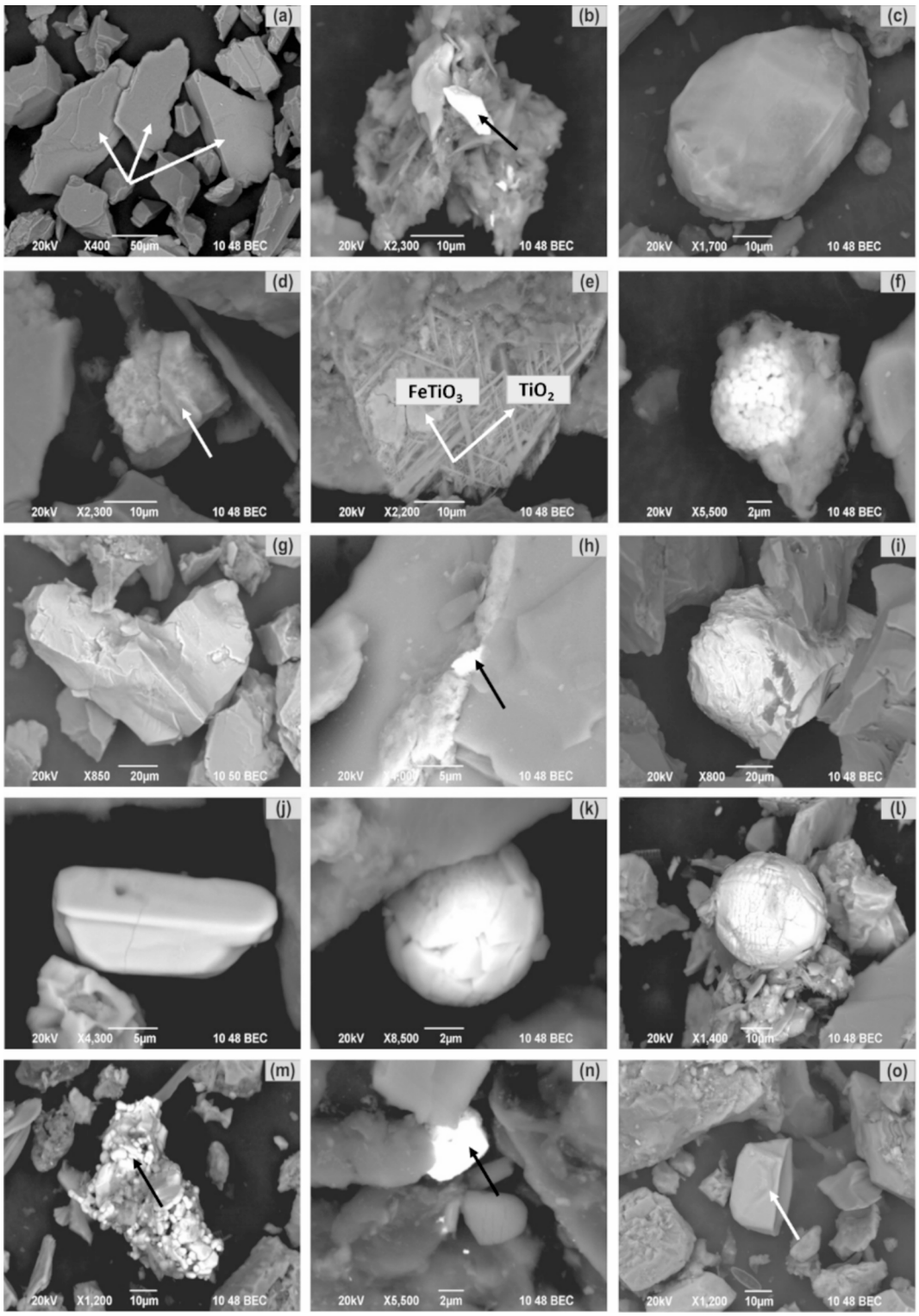

Fig. 6. SEM images of particles found in the Mura River catchment. Micrographs were made in BSE mode; a) micas, M–02b) barite, M−24; c) Cr–spinel, T–09; d) FeNi oxide/hydroxide, T–09; e) TiO_2 (probably rutile), ilmenite, M−15; f), pyrite, M−30; g) garnet group of minerals, M−15; h) xenotime group of minerals, T–01; i) monazite group of minerals, M−03 j) zircon, M−15; k) Fe–oxyhydroxide with a minor content of Zn, Cr, Cu, M−30; l) Fe–oxyhydroxide with minor content of Mn, M−24; m) Fe–oxyhydroxide with minor content of Cu and Zn, M−24; n) Pb sulphide, M−30; o) apatite, M−24.

subhedral particles in size of 30 μm (Fig. 6o). Elements associated with F7 are most probably associated withNa–plagioclases which have been commonly found throughout the river course, especially in samples of Zone 1.

4. Discussion

248 samples of stream and alluvial sediments from the Mura River were analysed for 59 elements using ICP–MS. The elemental levels determined in this study were compared with values determined by

Table 3
Median or mean levels in stream and alluvial sediments from the present and similar studies in European rivers.

element	unit	Stream sediments						Alluvial sediments					
		Mura	**Po**[1]	**Elbe**[2]	**Loire**[3]	**Danube**[4]	**EU**[5]	**Mura**	**Rhine**[6]	**Middle Rhone**[7]	**Drava**[8]	**Jizera**[9]	**EU**[5]
		Md	Md	Md	Avr	Avr	Md	Md	Avr	Md	Md	Md	Md
Al	%	7.2	9.7	3.5		7.2	10.3	7.8		1.42	6.8	4.02	10.4
As	mg/kg	11		17		18	6	17	14.2		16		6
Ba	mg/kg	415	232	340	512	489	386	521	301		480		379
Cd	mg/kg	0.23		0.63			0.28	0.26		0.14	0.5	1.2	0.3
Co	mg/kg	17	9	8.3		21	8	19			14		7
Cr	mg/kg	89	112	60		192	63	101		29.3	74	38	59
Cs	mg/kg	4.6		4.3		8.2	<4	6.2					4
Cu	mg/kg	31	21	21		91	17	37	17.1	18.4	28	74	17
Fe	%	4.5	3.56	2.4	6.34	4.2	3.57	4.7	1.98	2.17	3.8		3.33
Ga	mg/kg	17		12			12	19					11
Hf	mg/kg	0.52				5.2	8.3	0.48			0.50		4.51
K	%	1.6	1.55	1.3	2.04	1.8	2.01	1.9	1.21		1.6		2
Li	mg/kg	40					20.8	49			41		22.5
Mg	%	1.9	3.29	0.66		0.04	1.2	1.9			2.2		1.2
Na	%	1.5	0.96			0.86	0.9	1.4			1.1		0.8
Nb	mg/kg	12	7				13	9.21	5.2		8.9		10
Ni	mg/kg	49	59	20		101	21	60	24.6	32.7	34	37.1	22
Pb	mg/kg	28	16	36	81		20.5	40	26.1	17.7	53	26.8	22
Rb	mg/kg	80	81	66	164		70	99	67.3		83	78.4	71
Sc	mg/kg	17		6.5		14.8		17			12		
Sr	mg/kg	198	259	180	204	174	126	174	253		170		131
Th	mg/kg	12		12		12.2	10	11			11		8
Ti	%	0.53	0.4	0.36	0.89	0.55	0.625	0.43	0.22		0.39	0.23	0.48
Tl	mg/kg	0.43		0.51			0.39	0.61					0.37
U	mg/kg	2.5		3.2		2.2	2	2.4			2.3		2
V	mg/kg	114	94	55		121	62	124			97		56
Zn	mg/kg	100	77	140	195	327	71	120	45.6	64.6	140	93.4	65
Zr	mg/kg	18		130	266		391	14	114		13		215

*Md–median, Avr–average, 1 – Migani et al., 2015 (median values calculated based on medians of 7 different wetlands within the historical Po deltaic system), 2–Reese et al., 2019, 3 – Negrel, 1997, 4 – Culicov et al., 2021, 5 – Salminen et al., 2005, 6 – Berner et al., 2012 (mean values of upper layer are used; 21–69 cm), 7 – Dendievel et al., 2020, 8 – Šajn et al., 2011, 9 –Matys Grygar et al., 2013.

other studies of the European rivers (Table 3). Compared to the European median values ($EF_{EU} > 3$) for stream and floodplain sediments, sediments from the study area are enriched with As, Co, Cr, Cu, Mo, Ni and Sb (Table S2, Fig. 2) which is most probably due to the lithological composition of the catchment area and historic mining activities in the upper part of the river (Schmid et al., 2013; Fig. 1). Sb anomalies in this area, which were identified in the FOREGS project, were attributed to ore deposits and ancient mining and smelting activities (Salminen et al., 2005). Apart from Sb, FOREGS also identified elevated levels of Ce, Cr, Nb, Ta and W in this particular area, which are associated with Variscan granite and metamorphic rocks, such as those in the Kraubath area in the vicinity of point T–09 (Fig. 1). The comparison of median values of this study with medians or mean values of other European river sediments e.g. Elbe, Danube, and Rhine, did not reveal any significant deviations. However, the Hf and Zr values in Mura stream and alluvial sediments are significantly lower compared to the sediments of other European rivers. This can be most probably attributed to the incomplete (near–total) digestion method used in this study, in comparison to the total elemental determination by XRF used in studies of Reese et al. (2019), Negrel (1997). This is also in agreement with the studies of Okina et al. (2016) and Yu et al. (2001), which also report lower Zr and Hf levels due to incomplete digestion of samples.

Values of chemical elements are generally higher in smaller fractions compared to coarser ones, which is in line with the previous studies showing that heavy metal levels increase with decreasing particle size (Yao et al., 2015; Žibret, 2022). Higher contents of certain chemical elements in smaller fractions can be explained by their larger surface area per unit mass, which increases their adsorption capacity. This is also due to the presence of secondary minerals such as Fe, Mn, Al oxides and hydroxides, carbonates, and clay minerals. The coarser fractions, however, consist mainly of primary minerals such as quartz, which has a lower tendency to adsorb heavy metals (Hardy and Cornu, 2006; Yao et al., 2015).

Weathering of the parent material strongly influences the geochemical composition of sediments (Saha et al., 2023; Wu et al., 2013). The degree of the weathering process, and consequently the provenance of sediments, was determined using different weathering indexes such as CIA, PIA, and ICV (Table S3, Fig. 3). The CIA values of the Mura River sediments range from 53 to 71 with an average of 62, indicating low to moderate chemical weathering. Comparing the CIA values in the different areas of the Mura catchment i.e. zones, an increasing trend in the downstream direction has been observed with the highest values characterized for the Zone 3. This was further confirmed with a ternary Al_2O_3, $CaO^* + Na_2O$, K_2O (A–CN–K) diagram. Low CIA values in the Zone 1 indicate the persistence of labile cations such as Ca^{2+}, Na^{2+}, and K^+ in mineral phases (Verma et al., 2022). Also, factors F1 and F7, which are loaded with K and Na, respectively, reach their highest scores in the Zone 1 (Fig. 4). In the stream sediments of the Zones 2 and 3 the primary minerals slowly decomposed, resulting in the gradual formation of secondary minerals such as clay minerals (Saha et al., 2023). This was also confirmed by XRD measurements in our study, showing that the highest abundance of muscovite/illite is found in sample M−39 (Table 2) from the Zone 3. Furthermore, CIA values and the A–CN–K diagram suggest that sediments of the Mura River have been derived from the source rock, i.e. metamorphic rocks, that have undergone less chemical weathering. The low degree of weathering of sediments, especially in the upper part of the river, was also confirmed by low PIA and high ICV values (Fig. 3), which indicates a low degree of silicate weathering and structural immaturity in clastic sediments, and corresponds to the findings of other studies (i.e. Verma et al., 2022). A slightly higher weathering process of stream sediments in the lower part of the river could also be associated with the presence of volcanic rocks which, compared to intrusive rocks, weather more easily (Saha et al., 2023). To properly address the weathering status of sediments it is also necessary to address the weathering status of source rocks, which was not done in this study, but can be investigated in the future.

Seven geochemical associations were determined by factor analysis. F1 (K, Ba, Rb, Ga, Li, Tl, Cs, Be, Al, Cu, V) is mostly loaded with alkali metals (e.g. Li, K) and alkaline earth metals (e.g. Ba, Be) which are generally highly soluble (Dupré et al., 1996). F1 can indicate the erosion process of fresh igneous and metamorphic rocks in zones 1 and 2, and the deposition of mica, clay, and other similar minerals in the Zone 3. The highest F1 scores in the stream and alluvial sediments are found in the Zone 1, where high–grade metamorphic rocks of Tauern window, enriched with K–felspars, garnets, micas, and hornblendes, predominate (Schmid et al., 2013). The mineralogical characteristics of such samples in this study reveal a high abundance of muscovite, which is a K, Rb, and Li–rich mineral. The presence of micas was additionally confirmed by SEM/EDS (Fig. 6a). A slightly higher F1 score was also found in Leoben (M−16) and Mixnitz (M−20) and in a small fraction of alluvial sediments of profile P2 near Leoben. This increase in F1 scores is probably linked to the presence of barite as an accessory mineral in polymetallic Ag–Fe mineralization at Oberzeiring (Gaisberger et al., 2003) and Cu–Au mineralization at Flatschach (Gasser et al., 2009; Fig. 1). Carriers of barite were additionally identified by SEM/EDS (Fig. 6b).

F2 is loaded with Cr, Co, Ni, Mg, and V. The highest F2 scores were determined in the sediments of Mura's tributary – Chromwerkgrabenbach (Kraubath area), where mafic and ultramafic rocks can be found. Carriers of Cr and Ni in sediments from that area were also identified using SEM/EDS (Fig. 6c, 6d). Particles are occasionally slightly rounded which reflects a certain degree of fluvial transport (Walling and Woodward, 2000). Cr and Ni levels are compared to the ICV index, which can also show weathering resistance of sediments. Because Cr and Ni form very stable oxides it is expected that their levels might be higher in more weathering resistant materials. The results (Fig. 7) show that Cr and Ni levels in sediments are not linked with ICV index, with the exception of two tributaries slightly upstream of St. Michael in der Obersteiermark with the highest Cr and Ni levels also having the highest ICV index. This is highly likely linked with the nearby quarry operation in the Chromwerk, providing the influx of fresh sediment naturally enriched with Cr and Ni. Increased F2 score values in the wider area around Leoben could also be associated with anthropogenic factors, including winter sanding of roads, where the material from the serpentinite quarry of Kraubath area is used and the nearby steelworks. High levels of Cr and Ni in sediments in the area as a consequence of anthropogenic activities were also identified by the study of Irfan (2012). SEM/EDS analysis from this study also confirms the presence of particulate Cr–Ni alloys in sediments of tributary Gößbach (T–12), which is located in the intermediate vicinity of Leoben.

The highest F3 scores (Fe, Sc, Ti) were found in the Zone 2 and very likely correspond with the iron deposits, such as at Erzberg (Fig. 1) and other smaller iron deposits around Murau, Obdach, and Judenburg (Reismann, 2022), containing siderite ($FeCO_3$), ankerite ($CaFe[CO_3]_2$) and dolomite ($CaMg[CO_3]_2$) within the Paleosoic metamorphosed sedimentary rocks zone. Siderite deposits have been mined for more than 100 years to support the region's steel and iron industries. In this study, high Fe, Ti, and Sc levels in sediments were also found next to the former Fe mines. Specifically high values were detected in the coarser fraction of the Zederhausbach tributary (T–03) in Zone 1. Significantly high F3 scores were also detected downstream and upstream of Leoben in St. Michael in der Obersteiermark (M−15) and Niklasdorf (M−17; Fig. 4), probably reflecting the lithological composition of parent rocks of the region. Titanium is mostly related to natural occurrences of titanium minerals such as ilmenite, rutile, and spinel group as well as with titanium–bearing minerals, including perovskite and biotite (Milne and Fitzpatrick, 1977). Their sources are metamorphic rocks that are abundant in the area. Several Fe and Ti–bearing minerals (e.g. rutile, titanite, ilmenite, pyrite, Fe–rich garnets, and Fe–oxyhydroxides (pure and those with traces of PTEs; Fig. 6e–6g and 6k–6m)) were identified throughout the river course using SEM/EDS in this study. After the river crosses the town of Peggau (M−22), values of the F3 factor scores drop to around zero, except for a slight peak in the tributary Ščavnica (T–23). Levels of Fe were compared also with the CIA parameter to evaluate whether chemical alteration of sediments have an impact to Fe levels (Fig. 8). It is expected that higher weathered sediments might contain more Fe (as Fe^{3+}) as fresh sediments. Anthropogenic emissions of Fe–enriched materials from Fe mine, ironworks and metalworks might have high Fe levels, while at the same time low CIA value (low or no weathering). The results show that clear link between CIA and Fe content can be established, although the highest Fe levels were detected in moderately weathered sediments from tributaries.

Considering the aforementioned observations, the geochemical association represented by F3 reflects natural processes (weathering of Fe– and Ti–rich metamorphic rocks and ore deposits) and anthropogenic activities (provision of fresh sediments from mining, ironworking).

U, Th, and YREEs are loaded in F4. Levels of these elements are usually higher in pegmatites and other alkali rocks, which are abundant in Zone 1. REE–enriched minerals are relatively resistant to chemical

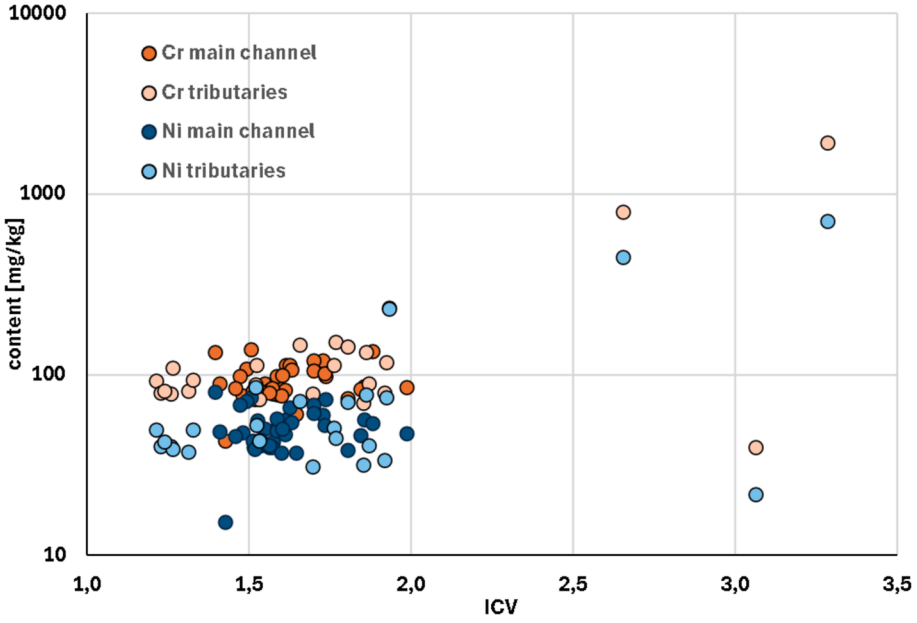

Fig. 7. Scaling of Cr and Ni levels in sediments with the index of compositional variability (ICV).

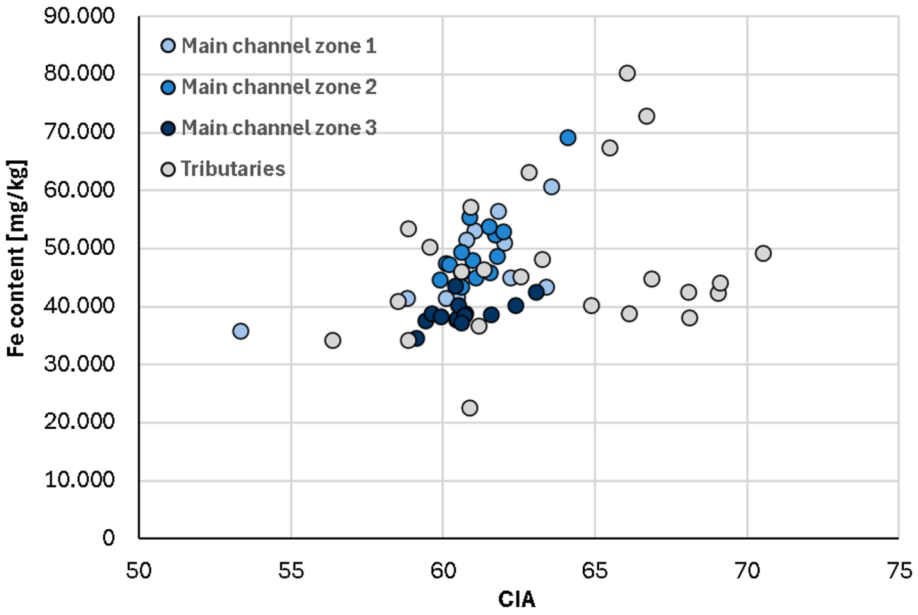

Fig. 8. Scaling of chemical index of alteration (CIA) and iron content in sediments.

weathering because REEs are not soluble (Wu et al., 2013). In this study, the highest values of F4 scores were found in Zone 1 next to the town Stadl an der Mur (M−07). This probably reflects the physical weathering of metamorphic rocks that are enriched with REE–bearing minerals. Their presence in this part of the study area was also confirmed with SEM/EDS (Fig. 6h, 6i). F4 scores steadily decrease downstream, especially in Zone 3, where alkali igneous rocks does not occur. The only exceptions are the sediments of tributary Sulm (T–23) that belong to Zone 3. This local increase in F4 scores might be linked to the presence of volcanic rocks, which are present in this region (Kralj, 2011).

F5 is loaded with Hf, Zr, Nb, and Ta, that generally form oxide minerals, which are resistant to chemical weathering, but their occurrence can be influenced by sorting of the river by their particle size and density (Wu et al., 2013). F5 values are low in the upper part of the Mura River but increase steadily downstream in stream (Fig. 4) and alluvial sediments (Fig. 5). The most common Zr– and Hf–bearing mineral is zircon which is a typical mineral of igneous and metamorphic rocks. Due to its fast crystallization from an igneous melt, zircon grains are often encased as inclusions in other minerals including feldspar or quartz (Pirkle and Podmeyer, 1998). Besides zircon, Zr also occurs as a trace element in other minerals including clinopyroxenes, amphiboles, micas, and garnets (Milne and Fitzpatrick, 1977), all of which are characteristic for the upper part of the Mura catchment. The reason for low values of F5 scores in zones 1 and 2, where the water energy is generally higher, and increased values of F5 scores in Zone 3, where water energy is lower, is most likely the erosion of Zr– and Hf– bearing minerals from zones 1 and 2 and their deposition in Zone 3. Similar results were also obtained by Saha et al. (2023), who found the presence of a significant amount of Zr in the lower part of the river as a result of the hydrodynamic transportation process. Such grains are normally present as a “heavy mineral fraction” within quartz sand, which, according to XRD analysis, predominates in the samples from the lower part of the river (M−39; Table 1). In this study, zircon grains were frequently identified using EDS analysis (Fig. 6j). F5 represents a natural geochemical association, linked to a heavy mineral fraction associated with erosional/depositional patterns.

F6 represents elements that are typical for anthropogenic contamination, such as Cd, In, Pb, and Zn, related to traffic (e.g. combustion, wear of brakes, tires (Benabdelkader et al., 2018; Gaberšek and Gosar, 2018; Teran et al., 2020)) and application of photovoltaic solar systems (Stamford and Azapagic, 2019). The highest values of F6 are found near urbanised areas (e.g. Graz (M−24), the largest city in the study area, Leoben (M−16), etc.; Fig. 4), especially in smaller fraction. The weathering indices, i.e. the CIA, also show different patterns for the Pb and Zn contents in highly urbanized and industrial areas (Fig. 7c). However, anomalies in this study occur only locally. Hanesch and Scholger (2002) also pointed out the elevated levels of some PTEs, including Cd and Zn, as a result of traffic and industry in the Mura catchment area. In this study, several PTE carriers (e.g. Zn, Cu, Pb) were detected by SEM/EDS in this study, mainly in sediments from Graz and downstream of Graz (Fig. 6k–6m). These particles often occur as 10–50 μm large, irregular conglomerates of smaller oval or spherical grains. The spherical morphology of pure Fe–oxyhydroxides or those with intrusions of PTEs usually indicates formation during melting in high–temperature processes, such as gas or oil combustion, followed by rapid cooling in the air, as also detected by Miler (2021) in urban sediments. In addition to the spherical particles, irregular particles of Fe–oxyhydroxides with a small proportion of trace and Cr–Ni alloys were also detected in this study. The wear of brake discs, pads or tyres is most likely the main source (Kukutschová et al., 2011; Miler, 2021). Pb and

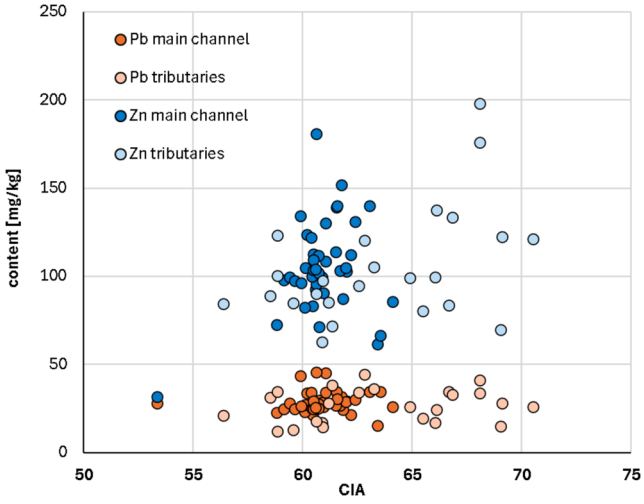

Fig. 9. Scaling of Pb and Zn levels in sediments with chemical index of alteration (CIA).

Zn levels were also compared with the corresponding CIA index value (Fig. 9). The results show that weathering has no influence on the Pb and Zn levels in the sediments, which might indicate that the origin of these two elements is not exclusively due to natural sources. In view of these observations, F6 can be attributed to anthropogenic activities, including traffic, combustion and similar.

It is also worth noting that several sedimentary exhalative (SEDEX) Pb–Zn–Ba deposits are known in the surroundings of Graz e.g., Arzwaldgraben as part of Paleozoic of Graz (Geringer et al., 2022; Weber, 1983), which could also explain increased values of F6 scores. SEM/EDS observation confirmed the presence of (naturally occurring) Pb sulphides (Fig. 6n) in the sediments in this area. The presence of Cd in this geochemical group can be further explained by the use of Cd–bearing fertilizers (P–rich fertilizers) in farming areas (Atafar et al., 2010; Kubier et al., 2019; Žibret and Čeplak, 2021), which are also developed around urban centres, although this study did not reveal a direct linkage. SEM/EDS analysis confirmed the presence of apatite minerals in the study area. Apatite is the primary source of phosphate in the fertilizers, that might also be carriers of Cd and other PTEs (Fig. 6o). The presence of geochemical association represented by F6 could be both of natural and anthropogenic origin, although the F6 occurrence distribution in the basin as well as the shape of grains by SEM/EDS indicate that anthropogenic origin is more probable.

Na and Sr are associated with F7, which is the last geochemical association detected in the study area. Locally increased values of F7 scores in tributaries are characteristic patterns of this association and are very likely linked to the presence of Na–rich plagioclases (i.e. albite), originating from igneous alkali rocks, which have also been confirmed by SEM/EDS. Sr could be an impurity in such minerals.

No significant or large–scale anthropogenic anomalies of PTEs in the sediments of the study area were detected. The obtained geochemical associations are of natural origin, such as weathering of source rocks, erosional and depositional patterns of the river and its tributaries, and variations in the mobility of certain elements. However, anthropogenic impacts can also be locally detected, caused by larger industries, urbanization, and possibly farming. The results of the study can be applied to many other similar areas globally, where various factors (present and historic) affecting the composition of river sediments interplay. However, this study did not address small–scale spatial and temporal variations, which could be the topic for further studies. Increased number of analysed samples can make observations from this study more reliable, and could also better define size and scale of anthropogenic influences.

The novelty of this study lies in its comprehensive approach to geochemical analysis, which combines elemental composition determination, factor analysis, X–ray diffraction, and SEM/EDS observations to elucidate the complex geochemical associations in fluvial sediments. This multifaceted methodology highlights the natural and anthropogenic influences on sediment composition andprovides a detailed classification of weathering processes and elemental anomalies within the Mura River system.

5. Conclusion

The geochemical associations in sediments from complex fluvial environments have been determined by analysing the elemental composition of 59 elements. This analysis utilized multivariate statistical methods such as factor analysis, and was further supported by X–ray diffraction and SEM/EDS observations. Determination of elemental composition of stream and alluvial sediments was done on two fractions (<0.063 mm and 0.063–0.125 mm). The sediments of the Mura River were classified as immature based on the CIA, PIA, and ICV values with the samples in the upper part of the river showing the lowest degree of weathering, while the sediments in the lower part of the river can be categorized as moderately weathered. The elemental composition of the Mura river sediments generally follows the various lithological characteristics of the catchment, however, anthropogenic anomalies of certain elements (e.g. Zn, Pb, Cd, Cr, and Ni) were also identified. Factor analysis showed the presence of seven geochemical associations of elements. Factor 1 (K, Ba, Rb, Ga, Li, Tl, Cs, Be, Al, Cu, and V) represents natural geochemical association connected mostly with the mica minerals. The second group of elements (Ni, Cr, Mg, Co, and V) is geogenically linked to the weathering of basic and ultrabasic rocks from the Kraubath area and anthropogenically to the steel industry around Leoben. Cr–Ni carriers (e.g., Cr–spinels) were identified. The third group (Fe, Ti, Sc) is both geogenic and anthropogenic, associated with iron ore bodies from Styria, iron ore mining and downstream industries. The representative minerals such as Fe–oxyhydroxides, TiO_2, pyrite, Fe–rich garnets, ilmenite, and titanite were identified. Factor 4 (Th, YREE, and U) is a natural association linked to the weathering of pegmatites and REE–rich minerals. Scores of F4 are significantly higher in the upper part of the river where high–grade metamorphic rocks predominate. Grains of monazite and xenotime groups of minerals were often detected in this area. The fifth geochemical association is also a natural one and consists of Zr, Hf, and Nb. It is linked to the heavy mineral fraction in quartz–rich sediments, deposited in the lower part of the river. Factor 6 (Zn, Pb, Cd and In) is most probably linked to anthropogenic activities, like urbanization, traffic, and agriculture. The highest F6 scores were detected in urban areas with highly developed industry, agriculture, and infrastructure. SEM/EDS analysis identified F6 element carriers, especially in the shape of Fe–oxyhydroxides. These particles often occur as irregularly–shaped agglomerates. The last identified geochemical association is again a natural one and consists of two elements: Na and Sr. This association is connected to Na–rich minerals e.g. Na–plagioclases (i.e. albite) and Na–pyroxenes which predominate in the upper part of the Mura River.

Declaration of competing interest

The authors declare that they have no known competing financial interests or personal relationships that could have appeared to influence the work reported in this paper.

Acknowledgements

This study was financially supported by the Slovenian Research and Innovation Agency (ARIS) and the Austrian Science Fund (FWF) within the research project MURmap (project number: I 5491, J1–3023), by the ARIS within the frame of the young researcher program, core funding programme P1–0025 “Mineral Resources” and P1–0034 “Analytics and Chemical Characterization of Materials and Processes”. We acknowledge the support of all local residents for granting access to sampling spots and their invaluable assistance.

Appendix A. Supplementary data

Supplementary data to this article can be found online at https://doi.org/10.1016/j.catena.2024.108605.

References

Atafar, Z., Mesdaghinia, A., Nouri, J., Homaee, M., Yunesian, M., Ahmadimoghaddam, M., Mahvi, A.H., 2010. Effect of fertilizer application on soil heavy metal concentration. Environ. Monit. Assess. 160, 83–89. https://doi.org/10.1007/s10661-008-0659-x.

Barandovski, L., Stafilov, T., Šajn, R., Frontasyeva, M., Andonovska, K.B., 2020. Atmospheric heavy metal deposition in North Macedonia from 2002 to 2010 studied by moss biomonitoring technique. Atmosphere (basel). 11, 1–23. https://doi.org/10.3390/atmos11090929.

Benabdelkader, A., Taleb, A., Probst, J.L., Belaidi, N., Probst, A., 2018. Anthropogenic contribution and influencing factors on metal features in fluvial sediments from a semi-arid Mediterranean river basin (Tafna River, Algeria): A multi-indices approach. Sci. Total Environ. 626, 899–914. https://doi.org/10.1016/j.scitotenv.2018.01.107.

Berner, Z.A., Bleeck-Schmidt, S., Stüben, D., Neumann, T., Fuchs, M., Lehmann, M., 2012. Floodplain deposits: A geochemical archive of flood history - A case study on

the River Rhine. Germany. Appl. Geochemistry 27, 543–561. https://doi.org/10.1016/j.apgeochem.2011.12.007.
Briffa, J., Sinagra, E., Blundell, R., 2020. Heavy metal pollution in the environment and their toxicological effects on humans. Heliyon 6, e04691.
Cheng, B.Y., Fang, W.T., Shyu, G.S., Chang, T.K., 2013. Distribution of heavy metals in the sediments of agricultural fields adjacent to urban areas in Central Taiwan. Paddy Water Environ. 11, 343–351. https://doi.org/10.1007/s10333-012-0325-3.
Cox, R., Lowe, D.R., Cullers, R.I., 1995. The influence of sediment recycling and basement composition on evolution of mudrock chemistry in the southwestern United States. Geochim. Cosmochim. Acta 59, 2919–2940. https://doi.org/10.1016/0016-7037(95)00185-9.
Culicov, O.A., Trtić-Petrović, T., Balvanović, R., Petković, A., Ražić, S., 2021. Spatial Distribution of multielements including technology critical elements in sediments of the Danube River. Environ. Sci. Pollut. Res. 28, 44877–44889. https://doi.org/10.1007/s11356-021-13752-6.
Dendievel, A.M., Mourier, B., Dabrin, A., Delile, H., Coynel, A., Gosset, A., Liber, Y., Berger, J.F., Bedell, J.P., 2020. Metal pollution trajectories and mixture risk assessed by combining dated cores and subsurface sediments along a major European river (Rhône River, France). Environ. Int. 144, 106032. https://doi.org/10.1016/j.envint.2020.106032.
Dupré, B., Gaillardet, J., Rousseau, D., Allègre, C.J., 1996. Major and trace elements of river-borne material: The Congo Basin. Geochim. Cosmochim. Acta 60, 1301–1321. https://doi.org/10.1016/0016-7037(96)00043-9.
Fedo, C.M., Wayne Nesbitt, H., Young, G.M., 1995. Unraveling the effects of potassium metasomatism in sedimentary rocks and paleosols, with implications for paleoweathering conditions and provenance. Geology 23, 921–924. https://doi.org/10.1130/0091-7613(1995)023<0921:uteopm>2.3.co;2.
Foucher, D., Ogrinc, N., Hintelmann, H., 2009. Tracing mercury contamination from the Idrija mining region (Slovenia) to the Gulf of Trieste using Hg isotope ratio measurements. Environ. Sci. Technol. 43, 33–39. https://doi.org/10.1021/es801772b.
Gaberšek, M., Gosar, M., 2018. Geochemistry of urban soil in the industrial town of Maribor. Slovenia. J. Geochemical Explor. 187, 141–154. https://doi.org/10.1016/j.gexplo.2017.06.001.
Gaberšek, M., Gosar, M., 2021. Towards a holistic approach to the geochemistry of solid inorganic particles in the urban environment. Sci. Total Environ. 763, 144214. https://doi.org/10.1016/j.scitotenv.2020.144214.
Gaisberger, G., Ebner, F., Prochaska, W., Sager, M., 2003. Environmental impact of historic mining and metallurgy to soils (Oberzeiring - Eastern Alps/Austria), in: Eliopoulos et al. (Ed.), Mineral Exploration and Sustainable Development. Millpress, Rotterdam, pp. 25–28.
Gasser, D., Gusterhuber, J., Krische, O., Puhr, B., Scheucher, L., Wagner, T., Stüwe, K., 2009. Geology of Styria: An overview. Mitteilungen Des Naturwissenschaftlichen Vereines Für Steiermark 139, 5–36.
Geringer, A., Rohrhofer, S., Melcher, F., Reither, H., Benold, C., Schuster, R., Auer, C., Paulick, H., Grasemann, B., Hubmann, B., Large, D., 2022. SEDEX deposits in the Graz Paleozoic - investigations to the exploration potential with the Arzberg deposit as calibration region. PANGEO Austria 2022 Abstr. F. Guid.
Globevnik, L., Mikoš, M., 2009. Boundary conditions of morphodynamic processes in the Mura River in Slovenia. Catena 79, 265–276. https://doi.org/10.1016/j.catena.2009.06.008.
Gosar, M., Žibret, G., 2011. Mercury contents in the vertical profiles through alluvial sediments as a reflection of mining in Idrija (Slovenia). J. Geochemical Explor. 110, 81–91. https://doi.org/10.1016/j.gexplo.2011.03.008.
Hanesch, M., Scholger, R., 2002. Mapping of heavy metal loadings in soils by means of magnetic susceptibility measurements. Environ. Geol. 42, 857–870. https://doi.org/10.1007/s00254-002-0604-1.
Hardy, M., Cornu, S., 2006. Location of natural trace elements in silty soils using particle-size fractionation. Geoderma 133, 295–308. https://doi.org/10.1016/j.geoderma.2005.07.015.
Hoffmann, T., Thorndycraft, V.R., Brown, A.G., Coulthard, T.J., Damnati, B., Kale, V.S., Middelkoop, H., Notebaert, B., Walling, D.E., 2010. Human impact on fluvial regimes and sediment flux during the Holocene: Review and future research agenda. Glob. Planet. Change 72, 87–98. https://doi.org/10.1016/j.gloplacha.2010.04.008.
Hossain, H.M.Z., Hasna Hossain, Q., Kamei, A., Araoka, D., 2018. Compositional variations, chemical weathering, and provenance of sands from the Cox's Bazar and Kuakata beach areas. Bangladesh. Arab. J. Geosci. 11. https://doi.org/10.1007/s12517-018-4111-4.
Irfan, M.I., 2012. Anthropogenic versus geogenic contamination of the Vordernbergerbach valley, Steiermark, Austria. A geochemical, mineralogical and geophysical study - Doctoral Thesis. Montanuniversität Leoben.
Kos, S., Zupančič, N., Gosar, M., Miler, M., 2022. Solid Carriers of Potentially Toxic Elements and Their Fate in Stream Sediments in the Area Affected by Iron Ore Mining and Processing. Minerals 12, 1424. https://doi.org/10.3390/min12111424.
Kralj, P., 2011. Eruptive and sedimentary evolution of the Pliocene Grad Volcanic Field, North-east Slovenia. J. Volcanol. Geotherm. Res. 201, 272–284. https://doi.org/10.1016/j.jvolgeores.2010.09.004.
Kubier, A., Wilkin, R.T., Pichler, T., 2019. Cadmium in soils and groundwater: A review. Appl. Geochemistry 108, 104388. https://doi.org/10.1016/j.apgeochem.2019.104388.
Kukutschová, J., Moravec, P., Tomášek, V., Matějka, V., Smolík, J., Schwarz, J., Seidlerová, J., Šafářová, K., Filip, P., 2011. On airborne nano/micro-sized wear particles released from low-metallic automotive brakes. Environ. Pollut. 159, 998–1006. https://doi.org/10.1016/j.envpol.2010.11.036.
Lychagin, M.Y., Tkachenko, A.N., Kasimov, N.S., Kroonenberg, S.B., 2015. Heavy Metals in the Water, Plants, and Bottom Sediments of the Volga River Mouth Area. J. Coast. Res. 31, 859–868. https://doi.org/10.2112/JCOASTRES-D-12-00194.1.
Matys Grygar, T., Nováková, T., Bábek, O., Elznicová, J., Vadinová, N., 2013. Robust assessment of moderate heavy metal contamination levels in floodplain sediments: A case study on the Jizera River. Czech Republic. Sci. Total Environ. 452–453, 233–245. https://doi.org/10.1016/j.scitotenv.2013.02.085.
McLennan, S.M., 1993. Weathering and global denudation. J. Geol. 101, 295–303. https://doi.org/10.1086/648222.
Meybeck, M., 1976. Total mineral dissolved transport by world major rivers. Hydrol. Sci. Bull. 21, 265–284. https://doi.org/10.1080/02626667609491631.
Migani, F., Borghesi, F., Dinelli, E., 2015. Geochemical characterization of surface sediments from the northern Adriatic wetlands around the Po river delta. Part I: Bulk composition and relation to local background. J. Geochemical Explor. 156, 72–88. https://doi.org/10.1016/j.gexplo.2015.05.003.
Miler, M., 2021. Airborne particles in city bus: concentrations, sources and simulated pulmonary solubility. Environ. Geochem. Health 43, 2757–2780. https://doi.org/10.1007/s10653-020-00770-5.
Mil-Homens, M., Costa, A.M., Fonseca, S., Trancoso, M.A., Lopes, C., Serrano, R., Sousa, R., 2013. Characterization of heavy-metal contamination in surface sediments of the minho river estuary by way of factor analysis. Arch. Environ. Contam. Toxicol. 64, 617–631. https://doi.org/10.1007/s00244-012-9861-5.
Milne, A.R., Fitzpatrick, R.W., 1977. Titanium and zirconium minerals, in: Dixon, B., Weed, S.B. (Eds.), Minerals in Soil Environments. Soil Science Society of America, Madison, pp. 1131–1205. Doi: 10.2136/sssabookser1.2ed.c23.
Negrel, P., 1997. Multi-element chemistry of Loire estuary sediments: Anthropogenic vs. natural sources. Estuar. Coast. Shelf Sci. 44, 395–410. https://doi.org/10.1006/ecss.1996.0139.
Nesbitt, H.W., Young, G.M., 1989. Formation and diagenesis of weathering profiles. J. Geol. 97, 129–147. https://doi.org/10.1086/629290.
Okina, O., Lyapunov, S., Avdosyeva, M., Ermolaev, B., Golubchikov, V., Gorbunov, A., Sheshukov, V., 2016. An Investigation of the Reliability of HF Acid Mixtures in the Bomb Digestion of Silicate Rocks for the Determination of Trace Elements by ICP-MS. Geostand. Geoanalytical Res. 40, 583–597. https://doi.org/10.1111/ggr.12124.
Pirkle, F.L., Podmeyer, D.A., 1998. Zircon: origin and uses. Soc. Mining. Metall. Explor. 292, 1–21.
Popov, S.I., Stafilov, T., Šajn, R., Tănăselia, C., Bačeva, K., 2014. Applying of factor analyses for determination of trace elements distribution in water from river Vardar and its tributaries. Macedonia/greece. Sci. World J. 2, 809253. https://doi.org/10.1155/2014/809253.
Pučko, E., Žibret, G., Teran, K., 2024. Comparison of elemental composition of surface and subsurface soils on national level and identification of potential natural and anthropogenic processes influencing its composition. J. Geochemical Explor. 258, 107422. https://doi.org/10.1016/j.gexplo.2024.107422.
Reczyński, W., Szarłowicz, K., Jakubowska, M., Bitusik, P., Kubica, B., 2020. Comparison of the sediment composition in relation to basic chemical, physical, and geological factors. Int. J. Sediment Res. 35, 307–314. https://doi.org/10.1016/j.ijsrc.2020.01.002.
Reese, A., Zimmermann, T., Pröfrock, D., Irrgeher, J., 2019. Extreme spatial variation of Sr, Nd and Pb isotopic signatures and 48 element mass fractions in surface sediment of the Elbe River Estuary - Suitable tracers for processes in dynamic environments? Sci. Total Environ. 668, 512–523. https://doi.org/10.1016/j.scitotenv.2019.02.401.
Reismann, B.A., 2022. Styrian Forests as a Basis of Mining Industry during the Middle Ages and Early Modern Times. Hist. Stud. Cent. Eur. 2, 45–68. https://doi.org/10.47074/hsce.2022-1.03.
Rieuwerts, J.S., Mighanetara, K., Braungardt, C.B., Rollinson, G.K., Pirrie, D., Azizi, F., 2014. Geochemistry and mineralogy of arsenic in mine wastes and stream sediments in a historic metal mining area in the UK. Sci. Total Environ. 472, 226–234. https://doi.org/10.1016/j.scitotenv.2013.11.029.
Saha, A., Roy, D.K., Khan, R., Ornee, T.I., Goswami, S., Idris, A.M., Biswas, P.K., Tamim, U., 2023. Provenance, weathering, climate and tectonic setting of Padma River sediments, Bangladesh: A geochemical approach. Catena 233, 107485. https://doi.org/10.1016/j.catena.2023.107485.
Šajn, R., Halamić, J., Peh, Z., Galović, L., Alijagić, J., 2011. Assessment of the natural and anthropogenic sources of chemical elements in alluvial soils from the Drava River using multivariate statistical methods. J. Geochemical Explor. 110, 278–289. https://doi.org/10.1016/j.gexplo.2011.06.009.
Salminen, R., Batista, M.J., Bidovec, M., Demetriades, A., De Vivo, B., De Vos, W., Gilucis, A., Gregorauskiene, V., Halamic, J., Heitzmann, P., Lima, A., Jordan, G., Klaver, G., Klein, P., Lis, J., Locutura, J., Marsina, K., Maxrecu, A., O'Conor, P.J., Olsson, S.A., Ottesen, R.T., Petersell, V., Plant, J.A., Reeder, S., Salpeteur, I., Sandstrom, H., Siewers, U., Steenfelt, A., Tarvainen, T., 2005. Geochemical Atlas of Europe. Part. 1, Background information, methodology and maps. Espoo : Geological Survey of Finland,.
Schimak, G., Dillinger, T., Wagner, H., 2005. Austria: The Process of Restructuring is Largely Complete, in: Müller, B., Finka, M., Lintz, G. (Eds.), Rise and Decline of Industry in Central and Eastern Europe. Springer, Berlin, Heidelberg, pp. 25–43. Doi: 10.1007/3-540-26695-x_2.
Schmid, S.M., Scharf, A., Handy, M.R., Rosenberg, C.L., 2013. The Tauern Window (Eastern Alps, Austria): A new tectonic map, with cross-sections and a tectonometamorphic synthesis. Swiss J. Geosci. 106, 1–32. https://doi.org/10.1007/s00015-013-0123-y.
Stamford, L., Azapagic, A., 2019. Environmental impacts of copper-indium-gallium-selenide (CIGS) photovoltaics and the elimination of cadmium through atomic layer deposition. Sci. Total Environ. 688, 1092–1101. https://doi.org/10.1016/j.scitotenv.2019.06.343.

Strojan, I., 2022. Vodnatost površinskih voda leta 2021. Ujma 36, 55–67.
Sutherland, R.A., 2000. Bed sediment-associated trace metals in an urban stream, Oahu. Hawaii. Environ. Geol. 39, 611–627. https://doi.org/10.1007/s002540050473.
Teran, K., Žibret, G., Fanetti, M., 2020. Impact of urbanization and steel mill emissions on elemental composition of street dust and corresponding particle characterization. J. Hazard. Mater. 384, 120963. https://doi.org/10.1016/j.jhazmat.2019.120963.
TIBCO Software Inc., 2020. Statistica.
Verma, M., Kanhaiya, S., Singh, B.P., Singh, S., 2022. Signatures of provenance, tectonics and chemical weathering in the Tawi River sediments of the western Himalayan Foreland. India. J. Sediment. Environ. 7, 425–441. https://doi.org/10.1007/s43217-022-00104-8.
Walling, D.E., Woodward, J.C., 2000. Effective particle size characteristics of fluvial suspended sediment transported by lowland British rivers. In: Publication, I.A.H.S. (Ed.), The Role of Erosion and Sediment Transport in Nutrient and Contaminant Transfer. Canada, pp. 129–139.
Weber, L., 1983. The Stratiform Lead-Zinc Mineralisation of the "Paleozoic of Graz" (Styria, Austria), in: Schneider, H.J. (Ed.), Mineral Deposits of the Alps and of the Alpine Epoch in Europe. Special Publication No. 3 of the Society for Geology Applied to Mineral Deposits. Springer, Berlin, Heidelberg, pp. 81–87. Doi: 10.1007/978-3-642-68988-8_9.
Wu, W., Zheng, H., Xu, S., Yang, J., Liu, W., 2013. Trace element geochemistry of riverbed and suspended sediments in the upper Yangtze River. J. Geochemical Explor. 124, 67–78. https://doi.org/10.1016/j.gexplo.2012.08.005.
Yao, Q., Wang, X., Jian, H., Chen, H., Yu, Z., 2015. Characterization of the particle size fraction associated with heavy metals in suspended sediments of the yellow river. Int. J. Environ. Res. Public Health 12, 6725–6744. https://doi.org/10.3390/ijerph120606725.
Yu, Z., Robinson, P., McGoldrick, P., 2001. An evaluation of methods for the chemical decomposition of geological materials for trace element determination using ICP-MS. Geostand. Newsl. 25, 199–217. https://doi.org/10.1111/j.1751-908x.2001.tb00596.x.
Žibret, G., 2022. Elemental Associations in Stream and Alluvial Sediments of the Savinja and Voglajna Rivers (Slovenia, EU) as a Result of Natural Processes and Anthropogenic Activities. Minerals 12, 861. https://doi.org/10.3390/min12070861.
Žibret, G., Čeplak, B., 2021. Distribution of Pb, Zn and Cd in stream and alluvial sediments in the area with past Zn smelting operations. Sci. Rep. 11, 17629. https://doi.org/10.1038/s41598-021-96989-y.
Žibret, G., Gosar, M., 2017. Multi-elemental composition of the Sava River sediments (Slovenia, EU). Environ. Earth Sci. 76, 501. https://doi.org/10.1007/s12665-017-6835-y.
Žibret, G., Rokavec, D., 2010. Household dust and street sediment as an indicator of recent heavy metals in atmospheric emissions: A case study on a previously heavily contaminated area. Environ. Earth Sci. 61, 443–453. https://doi.org/10.1007/s12665-009-0356-2.